The Contribution of In-situ and Ex-situ Star Formation in Early-Type Galaxies: MaNGA versus IllustrisTNG

Cannarozzo et al. 2022, arXiv:2210.08109, accepted MNRAS

ABSTRACT

We compare stellar mass surface density, metallicity, age, and line-of-sight velocity dispersion profiles in massive ($M_* \geq 10^{10.5}\,\mathrm{M}_\odot$) present-day early-type galaxies (ETGs) from the MaNGA survey with simulated galaxies from the TNG100 simulation of the IllustrisTNG suite. We find an excellent agreement between the stellar mass surface density profiles of MaNGA and TNG100 ETGs, both in shape and normalisation. Moreover, TNG100 reproduces the shapes of the profiles of stellar metallicity and age, as well as the normalisation of velocity dispersion distributions of MaNGA ETGs. We generally also find good agreement when comparing the stellar profiles of central and satellite galaxies between MaNGA and TNG100. An exception is the velocity dispersion profiles of very massive ($M_* \gtrsim 10^{11.5}\,\mathrm{M}_\odot$) central galaxies, which, on average, are significantly higher in TNG100 than in MaNGA ($\approx 50\,\mathrm{km\,s^{-1}}$). We study the radial profiles of *in-situ* and *ex-situ* stars in TNG100 and discuss the extent to which each population contributes to the observed MaNGA profiles. Our analysis lends significant support to the idea that high-mass ($M_* \gtrsim 10^{11}\,\mathrm{M}_\odot$) ETGs in the present-day Universe are the result of a merger-driven evolution marked by major mergers that tend to homogenise the stellar populations of the progenitors in the merger remnant.

Massive early-type galaxies (ETGs)の形成

- *in situ*: その銀河内部で形成された星
- *ex situ*: 銀河外部で形成された星 (merger)

➔ 銀河内部のradial structureに違いが出る
(stellar mass, metallicity, age, velocity dispersion)

➔ 観測(可視光IFS: MaNGA)と理論(simulation: IllustrisTNG TNG100)でETGsを選び出して比較し、形成過程を考える

- ここでETGsはg-r>0.6というカラーで選別

観測 vs 理論 & 理論でのin-situ vs ex-situ

- Stellar mass surface density: 理論と観測でよく一致。high massほどex-situ強い
- Stellar metallicity: 形状はおよそ一致、いくつかのケースでnormalizationが違う
  high-massではex-situの方が金属量高い ← 直前までcentral で今satellite
- Velocity dispersion:
  $M_*<10^{11.5}M_{sun}$: 観測の方がややsteepなプロファイル
  $M_*>10^{11.5}M_{sun}$: 全域にわたってTNG100の方が高い金属量
  lower massでは中心でex-situ(?)成分の速度分散が大きい
  ← ex-situ成分の表面密度が低いため？
- Age: 物理量を求めるコードにより不定性が大きい
  (age-metallicity degeneracyやコード内で使用しているテンプレートやageグリッド)

Central vs Satellite

- Mass, metallicity, Ageについては両者ともにMaNGAとTNG100がよく一致。
  in-situとex-situ成分の振る舞いも類似 ➔ satelliteもその直前まではcentralだった
- Velocity dispersion: satelliteはMaNGAとTNG100が一致
  centralではTNG100が全体に渡り50km/sも高い
  ← TNG100ではsubhaloの中心にDMが集中するため？

TNG100でのmergerの重要性

- Higher-mass ETGsでex-situ massの割合増加
- 特にmajor mergerの役割がhigher-mass ETGsほど増加
- Higher-massではmergerの経験数が多く、直近にmajor mergerをしている

➔ Massive systemはmajor mergerによって成長するシナリオを支持
⇔ 多くのminor mergerで成長するシナリオ

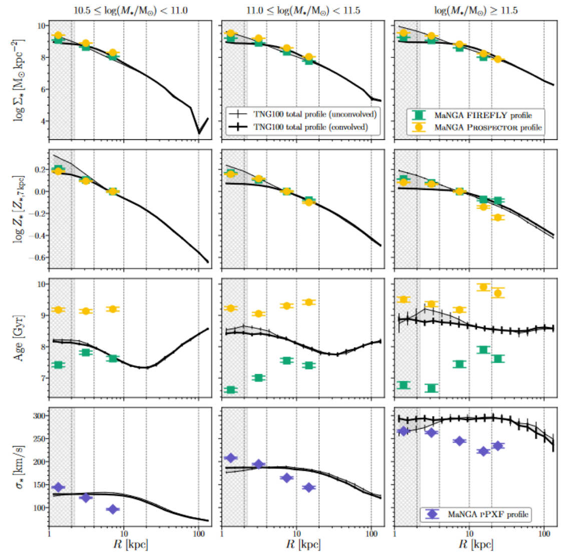

Figure 2. Radial profiles of stellar mass surface density, metallicity (normalised by the corresponding values of metallicity at ≈ 7 kpc), age, and line-of-sight velocity dispersion (from top to the bottom) in three bins of stellar mass for MaNGA and TNG100 ETGs. Green, yellow and violet dots represent the median estimates respectively for MaNGA galaxies from FIREFLY, Prospector and pPXF. Both the stellar metallicity and age measurements in MaNGA and TNG100 ETGs are mass weighted. Velocity dispersions are luminosity weighted for MaNGA and mass weighted for TNG100 sources. The vertical grey dashed lines indicate the 5 radial bins for MaNGA. The two black curves represent the median values of each stellar property for the total stellar population in TNG100. The intrinsic profiles are shown with the thin curve whereas the thick curves indicate the results when convolved with the MaNGA PSF. The light grey hatched area ($R \lesssim 2.1$ kpc) shows three times the gravitational softening length of the stellar particles in TNG100. The grey shaded area is the region that lies in between the profiles obtained from the original and the convolved TNG100 maps. Because we account for the MaNGA PSF but not for the effects of the resolution of the simulation, the grey shaded area gives a sense of the uncertainty in the comparison in the inner regions. The errorbars represent the 1σ uncertainties on the median for MaNGA and TNG100 estimates.

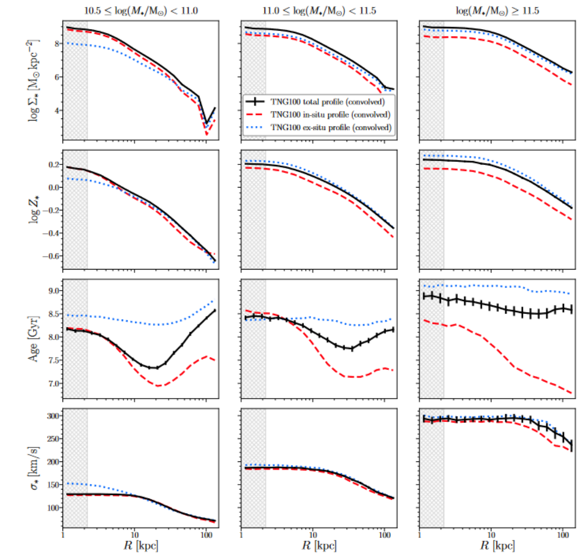

Figure 3. Contribution from in-situ and ex-situ stellar populations to the radial profiles of TNG100 ETGs. Top to bottom corresponds to profiles of stellar mass surface density, metallicity (not normalised), age, and line-of-sight velocity dispersion. The stellar metallicity, age, and velocity dispersion measurements are mass weighted. The black solid, red dashed, and blue dotted curves correspond to the total, in-situ, and ex-situ stellar populations, respectively. For clarity reasons, here we only show the median profiles convolved with the MaNGA PSF, and we omit the errorbars for the in-situ and ex-situ stellar population profiles. The light grey hatched area ($R \lesssim 2.1$ kpc) shows three times the gravitational softening length of the stellar particles in TNG100. *Note*: the range shown along the y-axes are different from those of Figure 2.

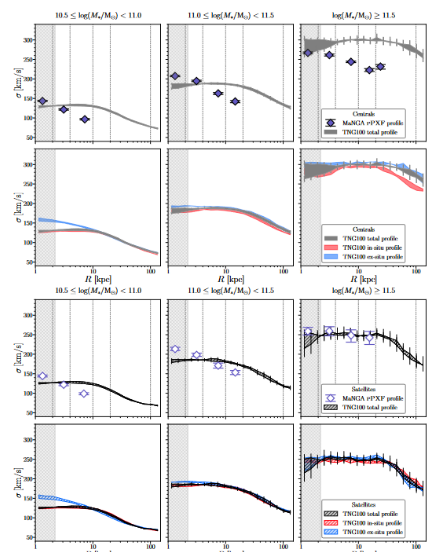

Figure 4. Line-of-sight stellar velocity dispersion radial profiles for centrals (upper rows) and satellites (lower rows). The violet-filled black and white-filled violet diamonds represent the median estimates of the mass-weighted velocity dispersion profiles for MaNGA central and satellite ETGs from pPXF code, respectively. The vertical grey dashed lines delimit the 5 radial intervals within stellar velocity dispersion is computed for MaNGA ETGs. The shaded and hatched areas represent the regions delimited by the median values of the mass-weighted velocity dispersion profiles obtained from the original TNG100 maps and the maps convolved with the MaNGA PSF for centrals and satellites, respectively. Black, red and blue colours correspond to the total, in-situ, and ex-situ stellar populations. For clarity reasons, we show only the errobars for the MaNGA and TNG100 total stellar population profiles. The light grey hatched area ($R \lesssim 2.1$ kpc) shows three times the gravitational softening length of the stellar particles in TNG100.

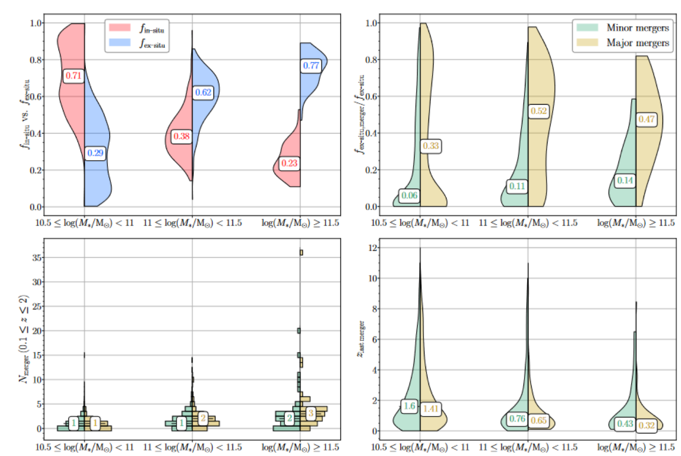

Figure 5. Data distributions of eight properties related to the merger histories of TNG100 ETGs. Top-left panel: total fractions of the in-situ (red distributions) and the ex-situ (blue distributions) stellar components. Top-right panel: fractions of the ex-situ stellar component from minor (green) and major (ocre) mergers normalised to the total ex-situ stellar fraction. Bottom-left panel: number of minor (green) and major (ocre) mergers across the redshift range $0.1 \leq z \leq 2$. Bottom-right panel: redshifts of the last minor (green) and major (ocre) mergers. All distributions are shown for the same three stellar mass bins as in Figure 2 and in Figure 3. Except for the number of minor and major mergers which are discrete values, the other properties are displayed as violin plots. For each property, the median value of the corresponding distribution is reported.